



## Mathematical study of the two-dimensional lasing problem for the whispering-gallery modes in a circular dielectric microcavity

ELENA I. SMOTROVA\* AND ALEXANDER I. NOSICH

*Institute of Radio-Physics and Electronics, NASU, Kharkov 61085, Ukraine*

(\*author for correspondence: E-mail: elena\_smotrova@yahoo.com)

**Abstract.** Microdisk lasers are investigated for their thresholds characteristics. We present a novel approach for studying the threshold gains of the whispering-gallery (WG) and other modes based on solving the boundary value problem for the Maxwell's equations. The novelty is that we consider the real-value pairs of frequencies and material gains as eigenvalues. In the two-dimensional (2D) approximation this problem is reduced to the set of independent transcendental equations. A Newton's method is further used to calculate the thresholds and natural frequencies numerically.

**Key words:** dielectric resonator, microdisk laser, threshold gain, whispering-gallery mode

### 1. Introduction

The laser, as a source of light, is a complicated device whose operation is based on the joint action and interplay of several physical mechanisms. The main are considered to be the transport of carriers, the quantum-mechanical stimulated emission, the processes of heating and cooling, and the optical (i.e., electromagnetic) field confinement. It is hard to simulate a laser with a model that takes full account of all these mechanisms, although this is the ultimate goal of the comprehensive modeling. Therefore, to reduce complexity, attention is normally paid to one of these effects neglecting the others. Here important place is occupied by the cold model associated with purely electromagnetic features of the laser as an open cavity containing an active material.

Since the pioneering research into lasers, a growing understanding had appeared that the cold-cavity modeling could bring extremely useful information on the lasing spectra. More recently this has been proven by the dozens of papers featuring modal analyses of VCSELs (Hadley *et al.* 1996; Burak and Binder 1997; Deng *et al.* 1997; Chang *et al.* 1998; Liu *et al.* 1998; Noble *et al.* 1998) and microcavity lasers (Frateschi and Levi 1995; Corbett *et al.* 1996; Li and Liu 1996; Sakai and Baba 1999; Fujita and Baba 2001). Here, a vast variety of approaches and methods have been tried: from

analytical descriptions in simple geometries (Frateschi and Levi 1995; Chang *et al.* 1998) to purely numerical ones with commercial FDTD solvers in the case of complicated boundaries and host media (Li and Liu 1996; Sakai and Baba 1999; Fujita and Baba 2001). Thorough inspection of these publications, however, reveals that all of them addressed the lasing indirectly, by studying the frequencies and  $Q$ -factors of the natural optical modes (i.e., electromagnetic modes able to exist in the absence of excitation) of the passive open resonators. FDTD studies are even further from the lasing effect, as they need a transient source placed into the cavity and evaluate  $Q$ -factors through the time-domain characteristics, instead of directly studying the complex-valued natural frequencies.

Semiconductor microdisks with quantum wells or boxes are of interest as potentially ultra-low-threshold laser devices. This is commonly attributed to the small volume of the cavity. Microlaser designs based on high-reflectivity WG modes around the edge of a thin semiconductor microdisk have been studied since the early 1990s (McCall *et al.* 1991; Frateschi and Levi 1995; Fujita *et al.* 1999). Here, the optical pump was normally arranged with a wide external laser beam (McCall *et al.* 1991; Frateschi and Levi 1995), hence the gain over the disk could be considered as uniform. The same, although less justified, was assumed for the injection lasers (Fujita *et al.* 1999). Still surprisingly, it appears that an accurate study of the circular-cavity lasing modes is absent, as the simplified analysis of (Frateschi and Levi 1995) was based on the rough assumptions, and FDTD simulations of (Fujita *et al.* 1999) dealt with the time-dependent excitation problems. Therefore such a full-wave Maxwellian analysis, within the 2D model, is our goal.

## 2. Eigenvalue problem formulation

The modes of a thin dielectric disk are complicated solutions to the 3D Maxwell equations. However, if the disk thickness is only a fraction of the wavelength the modes can be studied in the 2D formulation with the aid of the effective refraction index. Here, the bulk refraction index is replaced with the effective one, which depends on the material parameters, the thickness of resonator and the frequency (Buus 1984). This enables us to consider the lasing eigenvalue problem (LEP) for a circular resonator of radius  $a$  with a uniform refraction index and gain all along the cavity (Fig. 1) as a 2D model of the microdisk laser.

We look for the non-attenuating time-harmonic electromagnetic field  $\sim \exp(-ikt)$ ,  $k = \text{Re } k > 0$  in and out of a circular microcavity. Position in the cavity is specified by the axial, radial, and azimuth coordinates,  $z$ ,  $r$ ,  $\varphi$ . We assume that the field does not vary along the  $z$  axis and can be characterized by a scalar function  $U$ , which represents either  $E_z$  or  $H_z$  component

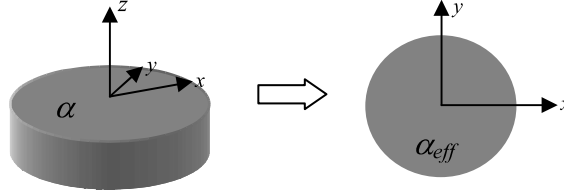


Fig. 1. Reduction of the disk electromagnetic problem to the 2D circular-cavity model.

depending on the polarization. Off the boundary, this function must satisfy the Helmholtz equation:

$$[\Delta + k^2 v^2(r, \varphi)]U(r, \varphi) = 0, \quad (1)$$

where step-wise function  $v(r, \varphi)$  is assumed 1 outside the cavity and a complex value inside:  $v = \alpha_{\text{eff}} - i\gamma$ , where  $\alpha_{\text{eff}} > 0$  is the effective refractive index and  $\gamma > 0$  is the material gain. The field must satisfy the continuity conditions across the boundary of resonator:

$$\begin{aligned} U^- &= U^+, \\ \frac{\partial U^-}{\partial r} &= \beta \frac{\partial U^+}{\partial r}, \end{aligned} \quad (2)$$

where  $\beta = 1$  if  $U = E_z$  or  $\beta = v^{-2}$  if  $U = H_z$ , and  $U^\pm = U(a \pm 0, \varphi)$ . In view of the real value of the wavenumber  $k$ , we impose the Sommerfeld radiation condition at infinity that selects outgoing field solutions:

$$\lim_{r \rightarrow \infty} \sqrt{r} \left( ik + \frac{\partial}{\partial r} \right) U(r, \varphi) = 0. \quad (3)$$

We shall consider the set of Equations (1)–(3) as an eigenvalue problem and look for the eigenvalues as pairs of real-valued parameters,  $(\kappa, \gamma)$ . The first of them is the normalized frequency of lasing,  $\kappa = ka$ , while the second is the threshold material gain.

This formulation is different from the ‘classical’ formulation of the eigenvalue problem for an open cavity, when the complex-valued frequency  $k$  is the eigenvalue parameter. In this case, the long-living natural oscillations with the higher  $Q$ -factors (i.e., smaller  $|\text{Im } k|$ ,  $\text{Im } k < 0$ ) are of the main interest; however the condition at infinity should be modified to permit the field growing up at  $r \rightarrow \infty$ . In the case of our formulation of LEP, there is no need of such admission of non-physical behavior (Nosich 2002). Besides, the threshold gain directly characterizes a laser operation while the  $Q$ -factor makes this indirectly.

### 3. Numerical results and discussion

We shall study the simplest LEPs for the modes in the GaAs/InAs microdisk assuming that the disk thickness is 200 nm and the lasing wavelength is  $\lambda = 1550$  nm. The effective refraction index is then 2.63 in the case of  $H_z$  polarization and 1.31 in the case of  $E_z$  polarization. As the effective refraction index of the  $E_z$ -polarized modes is only slightly greater than 1, the light emitted from a microdisk is always coupled to the  $H_z$ -polarized modes (Frateschi and Levi 1995). We shall consider both the  $E_z$  and  $H_z$  polarizations in detail and obtain the lasing frequencies and thresholds of the corresponding modes.

Separation of variables, assuming that  $U(r, \varphi) = R(r)\Phi(\varphi)$ , reduces the Helmholtz equation (1) to two independent differential equations

$$\frac{d^2 R}{dr^2} + \frac{1}{r} \frac{dR}{dr} + \left( v^2 k^2 - \frac{m^2}{r} \right) R = 0, \quad (4)$$

$$\frac{d^2 \Phi}{d\varphi^2} + m^2 \Phi = 0, \quad (5)$$

where  $m = 0, 1, 2, \dots$  and (4) is the Bessel differential equation.

Guided by these considerations and condition (3), we seek the field function as

$$U = \begin{cases} AJ_m(\kappa vr/a) \cos m\varphi, & r < a, \\ BH_m^{(1)}(\kappa r/a) \cos m\varphi, & r > a. \end{cases} \quad (6)$$

Therefore all the modes split into separate families according to the azimuth index  $m$ . Then the boundary conditions (2) lead to a set of independent transcendental equations for the eigenvalues in terms of the real and complex argument cylindrical functions of the integer index:

$$J_m(\kappa av)H_m^{(1)}(\kappa a) - \beta v H_m^{(1)}(\kappa a)J_m'(\kappa av) = 0. \quad (7)$$

We shall use another index,  $n = 1, 2, \dots$ , to number the eigenvalues within one family. We shall see that  $n$  will characterize the modal field variations along the disk radius.

The theory of complex variables tells that the set of eigenvalues  $(\kappa_{mn}, \gamma_{mn})$  is discrete; each of them may have only finite multiplicity; there are no finite accumulation points of eigenvalues in the plane  $(\kappa, \gamma)$ . Maxwell's equations guarantee that all  $\gamma_{mn} > 0$  (Nosich 2002).

Further we use 2-parametric Newton's method to obtain the eigenvalues numerically. Computation of the complex-argument Bessel functions presents no problem; this can be done with machine precision, for example, by the inverse-recursion algorithm (du Toit 1993).

Figs. 2 and 3 show the found eigenvalue pairs in the plane  $(\kappa, \gamma)$  within the strip  $0 < \kappa = ka < 13$ . One of the main points of the obtained results is that each  $m$ th family of modes displays two different types of behavior depending on the lasing frequency.

If  $m/\alpha < ka < m$ , then the modes are the WG ones and have exponentially small thresholds. This is explained by the quasi-total-reflection mechanism of the WG mode field forming. It is seen that the higher the azimuth index  $m$  of the lasing mode, the smaller the threshold gain. The smallest threshold in each family is observed for the  $WG_{m1}$  mode, whose  $E$ -field has a single maximum inside or near the cavity boundary. The type of the modal behavior changes as  $ka$  approaches  $m$ . If  $ka > m$ , much larger values of  $\gamma_{mn}$  are observed. Therefore we call corresponding modes as non-WG ones; in this range, the thresholds are inverse proportional to the lasing frequencies. In the case of the  $E_z$  polarization, all the thresholds of each  $m$ th family of modes are nearly inverse proportional to the lasing frequency due to the fact that the refractive index is only slightly greater than 1. For the very small cavities, namely if  $ka < m/\alpha$ , no lasing modes of the  $m$ th family can be found.

Each eigenvalue continuously depends on the refraction index  $\alpha$ . As one can see in Fig. 4, the thresholds and lasing frequencies get smaller with greater values of  $\alpha$ .

The modal field patterns of the circular microcavity are given by the expression (4), where  $\kappa = \kappa_{mn}$ ,  $v = \alpha_{\text{eff}} - i\gamma_{mn}$  and,  $A \equiv A_{mn} = BH_m^{(1)}(\kappa_{mn})/J_m(\kappa_{mn}v)$ .

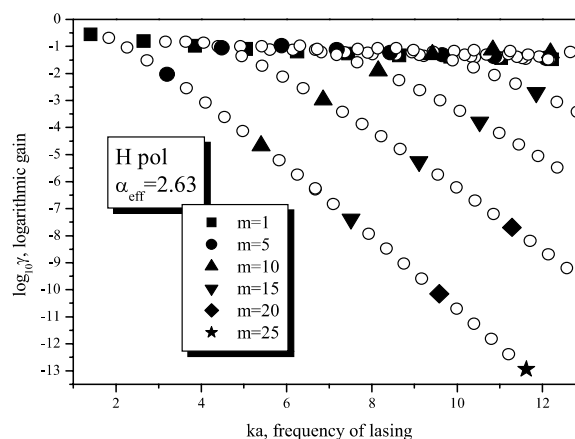


Fig. 2. Lasing spectra and thresholds of the  $H_z$ -polarized modes in a GaAs/InAs circular cavity.

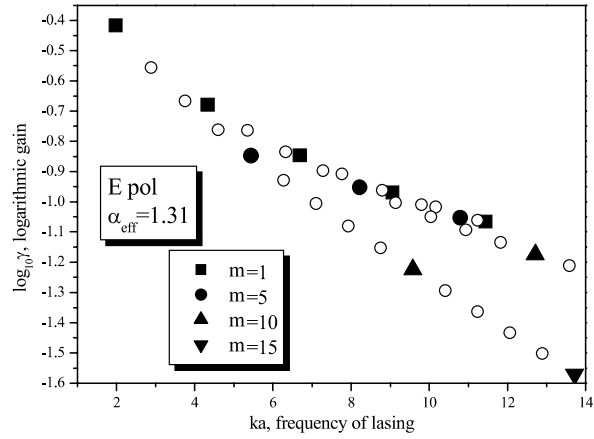


Fig. 3. Lasing spectra and thresholds of the  $E_z$ -polarized modes in a GaAs/InAs circular cavity.

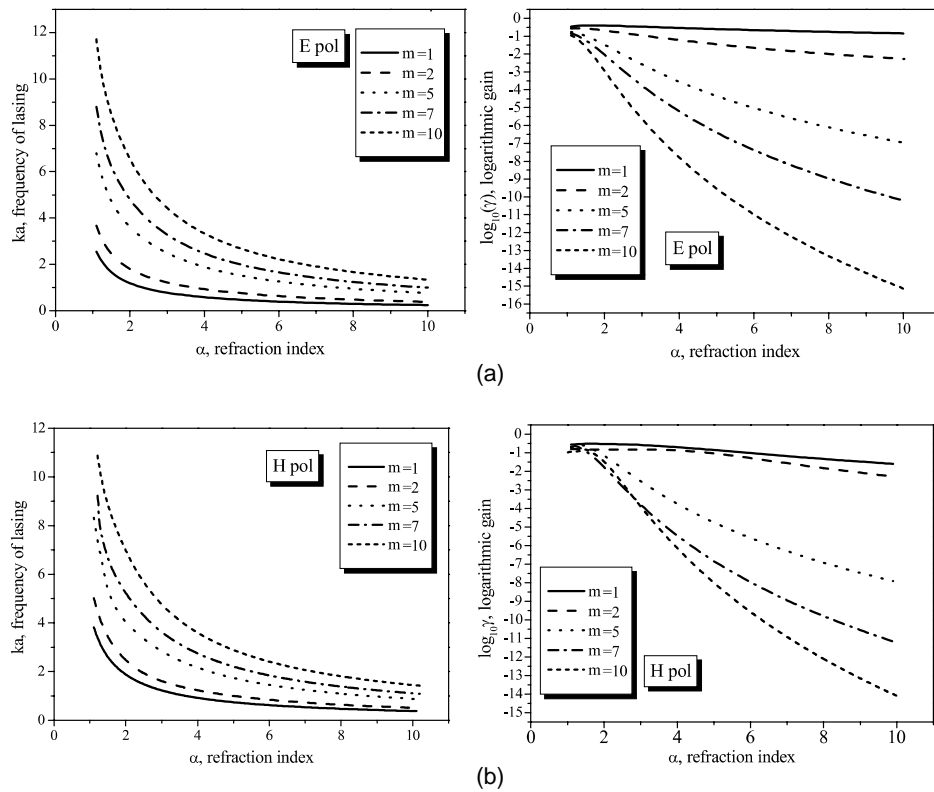


Fig. 4. Dependences of the characteristics of the  $WGE_{m1}$  (a) and  $WGH_{m1}$  (b) modes on the refraction index  $\alpha$ .

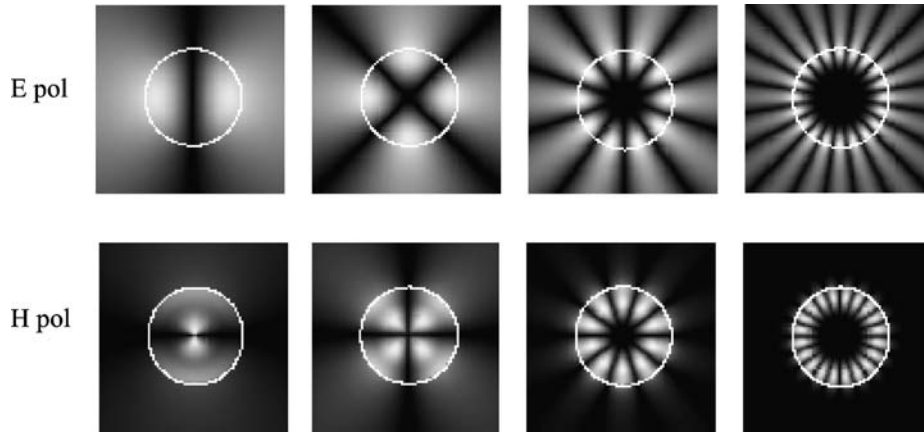


Fig. 5. Near  $E$ -field patterns: (a)  $E_{1,1}$ ,  $ka = 1.98$ ,  $\gamma = 0.38$ , (b)  $E_{2,1}$ ,  $ka = 2.9$ ,  $\gamma = 0.28$ , (c)  $E_{5,1}$ ,  $ka = 5.43$ ,  $\gamma = 0.14$ , (d)  $E_{10,1}$ ,  $ka = 9.58$ ,  $\gamma = 5.97 \times 10^{-2}$ , (e)  $H_{1,1}$ ,  $ka = 1.4$ ,  $\gamma = 0.28$ , (f)  $H_{2,1}$ ,  $ka = 1.8$ ,  $\gamma = 0.2$ , (g)  $WGH_{5,1}$ ,  $ka = 3.2$ ,  $\gamma = 9.3 \times 10^{-3}$ , (h)  $WGH_{10,1}$ ,  $ka = 5.4$ ,  $\gamma = 2.1 \times 10^{-5}$ .

Fig. 5 shows the near- $E$ -field intensities of the non-WG and WG modes of the both polarizations, for the mentioned GaAs/InAs disk. Once again one can clearly observe the difference in the  $E_z$  and  $H_z$ -polarized modes due to the different values of the effective refraction index.

Additionally, the cavity stability against the mode switching is a practically important parameter in the laser design. This quantity is determined by the relative threshold difference among the nearest modes. For example, for the modes of the same  $m$ th family,

$$s_{mn} = (\gamma_{mn} - \gamma_{mn'}) / \gamma_{mn}. \tag{8}$$

Fig. 6 shows stabilities for the modes of the several  $m$ th families of both polarizations. The modes with  $n = 1$  are the most stable in the  $H_z$  polarization

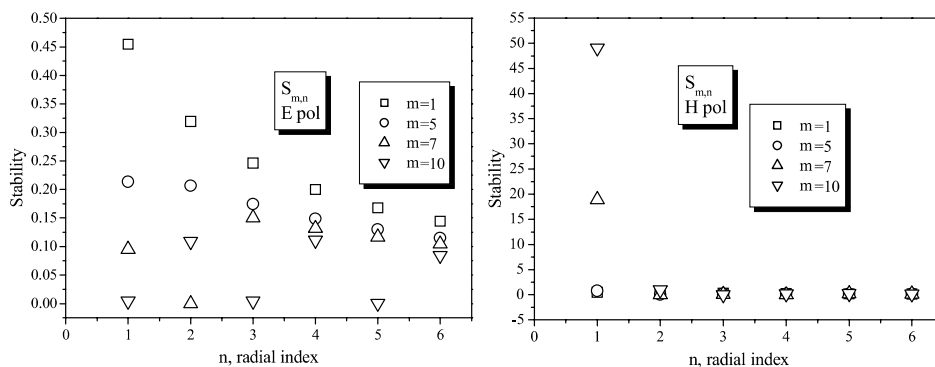


Fig. 6. The cavity stability against the mode switching.

while the less stable ones are those having  $\kappa_{mn} \approx m$ . In the case of the  $E_z$  polarization the modes with  $n = 1$  loose stability with growing index  $m$  due to the small index difference between the disk material and surrounding air.

#### 4. Conclusions

We have studied the LEPs for the  $E_z$  and  $H_z$ -polarized modes in a circular dielectric microcavity as the 2D model of a realistic GaAs/InAs microdisk laser. This cold-cavity analysis has revealed that, unlike previously published observations, not all the modes of the disk are automatically the WG ones. More precisely, the free spectral range (the distance between the nearest modes in frequency) is nearly the same for all modes of each  $m$ th family and depends mainly on the cavity radius and its effective refraction index. However, in terms of thresholds the WG and non-WG modes display very different behavior. The WG modes, whose near-field patterns are governed by the quasi-total-reflection mechanism, have exponentially small thresholds getting down with the azimuth index  $m$ . Non-WG modes have drastically higher thresholds coupled to the frequencies by a hyperbolic relation. The ranges of the WG and non-WG mode spectra are approximately divided by the value  $\kappa_{mn} \approx m$ , thus  $m\alpha^{-1} < 2\pi a\lambda_{mn}^{-1} < m$  for the WG modes and  $m < 2\pi a\lambda_{mn}^{-1}$  for the non-WG ones. In each  $m$ th family of the either polarization, the  $WG_{m1}$  ( $n = 1$ ) mode is the most stable and has the lowest threshold. In the range  $\kappa < m/\alpha$ , lasing modes are not found. Based on the presented analysis, we can conclude that the ultra-low material-gain thresholds of the  $H_z$ -polarized WG modes are explained by the almost total internal reflection rather than only by a low volume of the laser cavity. Note that, as our cavity is axially symmetric, all the orthogonal modes having  $m > 0$  are twice degenerate. In other words, optical modes with  $\cos m\varphi$  replaced with  $\sin m\varphi$  in (6) have the same lasing spectra and thresholds.

Finally, we would like to emphasize that the thresholds obtained from the LEP analysis cannot be simply transformed to the  $Q$ -factors or the radiation losses (given by  $\text{Im} k_{mn}$ ) of the ‘classical’ eigenvalue problem. The reason is that the parameter  $\nu$  is present not only in the Helmholtz equation (1), where it enters as a product with wavenumber  $k$ , but also in the boundary conditions (2). However, an ‘asymptotic’ observation takes place for the very high- $Q$  modes: the higher  $Q$ -factor, the lower the threshold.

#### References

- Burak, D. and R. Binder. *IEEE J. Quantum Electron.* **33** 1205, 1997.  
 Buus, J. *IEEE J. Quantum Electron.* **20** 1106, 1984.

- Chang, K.Y., J. Woodhead and P.N. Robson. *Appl. Phys. Lett.* **72** 335, 1998.
- Corbett, B., J. Justice, L. Cosidine, *et al.* *IEEE Photonic Technol. Lett.* **8** 855, 1996.
- Deng, Q., D.G. Deppe, *et al.* *IEEE J. Quantum Electron.* **33** 2319, 1997.
- du Toit, C.F. *IEEE Antennas Propag. Mag.* **35** 19, 1993.
- Frateschi, N.C. and A.F. Levi. *Appl. Phys. Lett.* **66** 2932, 1995.
- Fujita, M. and T. Baba. *IEEE J. Quantum Electron.* **37** 1253, 2001.
- Fujita, M., A. Sakai and T. Baba. *IEEE J. Select. Topics Quantum Electron.* **5** 673, 1999.
- Hadley, G.R., *et al.* *IEEE J. Quantum Electron.* **32** 607, 1996.
- Li, B.J. and P.L. Liu. *IEEE J. Quantum Electron.* **32** 1583, 1996.
- Liu, G., J.-F. Seurin, *et al.* *Appl. Phys. Lett.* **73** 726, 1998.
- McCall, S.L., A.F. Levi, R.E. Slusher, *et al.* *Appl. Phys. Lett.* **60** 289, 1991.
- Noble, M.J., J.P. Loehr and J.A. Lott. *IEEE J. Quantum Electron.* **34** 1892, 1998.
- Nosich, A.I. *Proc. Int. Conf. NUSOD, Zurich*, 76, 2002.
- Sakai, A. and T. Baba. *J. Lightwave Technol.* **17** 1439, 1999.